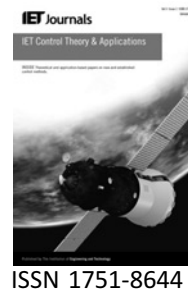


Published in IET Control Theory and Applications
 Received on 17th June 2008
 Revised on 18th October 2008
 doi: 10.1049/iet-cta.2008.0243



Position control of permanent magnet stepper motors using conditional servocompensators

S. Seshagiri

ECE Department, San Diego State University, San Diego, CA, USA
 E-mail: seshagir@engineering.sdsu.edu

Abstract: The application of the ‘conditional servocompensator’ technique to position control of a permanent magnet stepper motor is studied. This is a recent approach to the output regulation of minimum-phase non-linear systems that results in better transient performance over ‘conventional’ servocompensator-based design. Global regulation results are provided for state-feedback control and semi-global results under output feedback, with regional results when the control is constrained. The simulation results show that good tracking performance is achieved, in spite of partial knowledge of the machine parameters.

1 Introduction

Permanent magnet stepper motors (PMSM) have become a popular alternative to the traditionally used brushed DC motors (BDCM) for many high performance motion control applications for several reasons: better reliability because of the elimination of mechanical brushes, better heat dissipation as there are no rotor windings, higher torque-to-inertia ratio because of a lighter rotor, lower price and easy interfacing with digital systems [1]. They are now widely used in numerous motion control applications such as robotics, printers, process control systems and so on. Some of the drawbacks of PM machines when operated in open loop are the occurrence of large overshoots and settling times, especially when the load inertia is high, and the fact that microstepping is not possible in the open-loop mode of operation. As a result, over the years, many control algorithms that can improve the performance of PMSMs in a closed-loop operation have been examined.

Zribi and Chiasson [2] used the technique of exact feedback linearisation using full state-feedback, with extensions to the partial state-feedback case in [3, 4], and experimental validation of the controller in [3]. Adaptive solutions to the problem, under varying assumptions on the measurable states and on what parameters in the system are partially or wholly known, have appeared, for example, in the works of Dawson and co-workers [1, 5], Khorrami and co-workers [6–9] and others [10]. A sliding mode controller (SMC) along with

implementation results was reported in Zribi *et al.* [11]. In order to avoid the chattering problem associated with the ‘static’ discontinuous SMC, a ‘dynamic’ or ‘second-order’ SMC was proposed, where the discontinuities were relegated to the derivatives of the control input.

We present a new approach to position control based on a recently proposed technique for the output regulation of minimum-phase non-linear systems [12, 13], which incorporates a servocompensator as part of a robust SMC design. The servocompensation is ‘conditional’ in the sense that it behaves like a servocompensator only inside the boundary layer. This is shown to improve the transient performance over conventional servocompensator design. The method applies to MIMO non-linear systems with well-defined relative degree, which are transformable to normal form uniformly in a compact set of unknown parameters, and minimum phase. The design guarantees global regulation under state-feedback semi-global regulation under output-feedback and regional regulation with constrained control, under slightly differing assumptions. The performance of the design is comparable to ideal (discontinuous) SMC, but does not suffer from the drawback of chattering. In the special case of constant exogenous signals, the conditional servocompensator can be simplified to specially tuned PI/PID controllers with an anti-windup structure (see [12, Section 6]) for relative degree one and two systems respectively. Preliminary results were presented in our earlier work [14].

The rest of this paper is organised as follows. The system model is presented in Section 2, and Section 3 deals with conditional integrator design for the case of (asymptotically) constant exogenous signals, with the design done for both the state and output-feedback cases. An extension to the case of sinusoidal reference signals using conditional servocompensators is presented in Section 4, and conclusions are presented in Section 5. The specific contribution of this work over [14] are the results of Section 4.1, dealing with internal model perturbations, and the advantages of the proposed (conditional servocompensator) approach over a conventional approach in handling such perturbations.

2 System model

A schematic of a PMSM that has a slotted stator with two phases, and a PM rotor is shown in Fig. 1.

The mathematical model of the PMSM is given below [2, 3, 11]

$$\left. \begin{aligned} \frac{di_a}{dt} &= \frac{1}{L}(v_a - Ri_a + K_m \omega \sin(N_r \phi)) \\ \frac{di_b}{dt} &= \frac{1}{L}(v_b - Ri_b + K_m \omega \cos(N_r \phi)) \\ \frac{d\omega}{dt} &= \frac{1}{J}(K_m i_b \cos(N_r \phi) - K_m i_a \sin(N_r \phi) - B\omega - \tau_L) \\ \frac{d\phi}{dt} &= \omega \end{aligned} \right\} (1)$$

where i_a is the current in winding A, i_b is the current in winding B, ϕ is the angular displacement of the shaft of the motor, ω is the angular velocity of the shaft of the motor, v_a is the voltage across winding A, v_b is the voltage across winding B, N_r is the number of rotor teeth, J is the rotor and load inertia, B is the viscous friction coefficient,

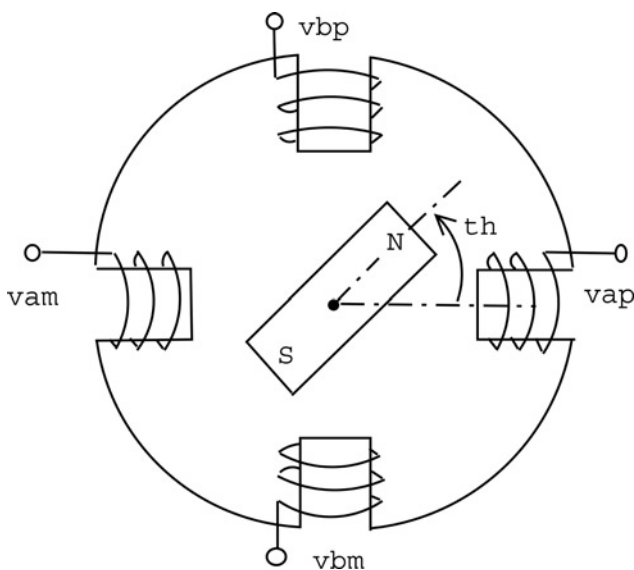


Figure 1 Schematic of a two-phase PMSM

L and R are the inductance and resistance, respectively, of the phase windings, K_m is the motor torque (back-emf) constant, and τ_L is the load torque. The model neglects the slight magnetic coupling between the phases, the small change in inductance as a function of the rotor position, the detent torque [6], and the variation in inductance because of magnetic saturation. The DQ transformation [2] from the fixed axes variables (x_a, x_b) to the dq axes variables (x_d, x_q) , defined by

$$\begin{bmatrix} x_d \\ x_q \end{bmatrix} \stackrel{\text{def}}{=} \begin{bmatrix} \cos(N_r \phi) & \sin(N_r \phi) \\ -\sin(N_r \phi) & \cos(N_r \phi) \end{bmatrix} \begin{bmatrix} x_a \\ x_b \end{bmatrix}$$

changes the frame of reference from the fixed phase axes to axes that are moving with the rotor. The direct current i_d corresponds to the component of the stator magnetic field along the axis of the rotor magnetic field, whereas the quadrature current i_q corresponds to the orthogonal component. Defining the states, inputs and outputs as

$$\begin{aligned} x_1 &= i_d, & x_2 &= i_q, & x_3 &= \omega, & x_4 &= \phi, & u_1 &= v_d, \\ u_2 &= v_q, & y_1 &= i_d, & \text{and } y_2 &= \phi \end{aligned}$$

it can be verified that (1) can be rewritten in the form of the following state model for the PMSM

$$\begin{aligned} \dot{x}_1 &= -k_1 x_1 + k_5 x_2 x_3 + k_6 u_1 \\ \dot{x}_2 &= -k_1 x_2 - k_5 x_1 x_3 - k_2 x_3 + k_6 u_2 \\ \dot{x}_3 &= k_3 x_2 - k_4 x_3 - d_0 \\ \dot{x}_4 &= x_3 \\ y_1 &= x_1 \\ y_2 &= x_4 \end{aligned} \quad (2)$$

where the constants k_1-k_6 and d_0 are related to N_r, J, B, L, R, K_m and τ_L by

$$\begin{aligned} k_1 &= \frac{R}{L}, & k_2 &= \frac{K_m}{L}, & k_3 &= \frac{K_m}{J}, & k_4 &= \frac{B}{J}, & k_5 &= N_r, \\ k_6 &= \frac{1}{L} & \text{and } d_0 &= \frac{\tau_L}{J} \end{aligned}$$

3 Conditional integrator design

We consider the case of asymptotically constant exogenous signals, that is, it is desired that the rotor angular position and direct-axis current track given references $\phi_d(t)$ and $I_{dd}(t)$ that tends to constant values as $t \rightarrow \infty$ [11]. It can be verified that the system (2) has full vector relative degree $\rho = \{1, 3\}$, globally in R^4 . In ideal sliding mode control, a choice of sliding surface functions would have been

$$\begin{aligned} s_1 &= e_1, & e_1 &\stackrel{\text{def}}{=} y_1 - I_{dd}, \\ s_2 &= k_1^2 e_2 + k_2^2 \dot{e}_2 + \ddot{e}_2, & e_2 &\stackrel{\text{def}}{=} y_2 - \phi_d \end{aligned} \quad (3)$$

with k_1^2 and k_2^2 chosen such that the polynomial

$$\lambda^2 + k_2^2\lambda + k_1^2$$

is Hurwitz, and the control designed to force the trajectories to reach the surfaces $s_i = 0$ in finite time and remain on them thereafter. However, as is well known, this method suffers from the drawback of chattering, and can excite unmodelled high-frequency dynamics and degrade system performance. Replacing the discontinuous (ideal) control by a continuous approximation in a boundary layer of the sliding surface reduces chattering but at the expense of a finite steady-state error. Asymptotic regulation can be recovered in the continuous sliding mode control (CSMC) by augmenting a conventional integrator

$$\dot{\sigma}_i = e_i$$

as part of the sliding surface but (i) requires a redesign of the sliding surface parameters and (ii) degrades transient performance in comparison to ideal SMC, in part because of the increase in system order as a result of the integrator, and in part because of the interaction of the integrator with control saturation, which leads to the well known problem of windup. In [12], we presented a ‘conditional integrator’ design that introduces integral action conditionally, that is, only inside the boundary layer, thereby recovering asymptotic regulation of ideal SMC, while not degrading its transient performance. The design in [12] was presented for a general MIMO non-linear system, modelled by

$$\begin{aligned} \dot{x} &= f(x, \theta) + \sum_{i=1}^m g_i(x, \theta)[u_i + \delta_i(x, \theta, w)] \\ y_i &= b_i(x, \theta), \quad 1 \leq i \leq m \end{aligned}$$

with state $x \in R^n$, input $u \in R^m$, output $y \in R^m$, θ a vector of unknown constant parameters belonging to the compact set $\Theta \subset R^p$, $w(t)$ a piecewise continuous exogenous signal belonging to a compact set $W \subset R^q$, $f(\cdot)$ and $g_i(\cdot)$ smooth vector fields, and piecewise continuous disturbances $\delta_i(\cdot)$. In the rest of this section, we directly present the design in [12] for the PMSM model (2).

3.1 State-feedback design

In order to recover the asymptotic regulation of ideal SMC and also retain its transient performance, we modify the sliding surfaces (3) as follows

$$\begin{aligned} s_1 &= k_0^1\sigma_1 + e_1 \\ s_2 &= k_0^2\sigma_2 + k_1^2e_2 + k_2^2\dot{e}_2 + \ddot{e}_2 \end{aligned} \quad (4)$$

where σ_1 and σ_2 are the outputs of the conditional

integrators

$$\begin{aligned} \dot{\sigma}_1 &= -k_0^1\sigma_1 + \mu_1\text{sat}(s_1/\mu_1), \quad \sigma_1(0) \in [-\mu_1/k_0^1, \mu_1/k_0^1] \\ \dot{\sigma}_2 &= -k_0^2\sigma_2 + \mu_2\text{sat}(s_2/\mu_2), \quad \sigma_2(0) \in [-\mu_2/k_0^2, \mu_2/k_0^2] \end{aligned} \quad (5)$$

$k_0^1, k_0^2 > 0$, the values of k_1^2 and k_2^2 are retained from the ideal SMC design (3), and μ_1, μ_2 are ‘sufficiently small’ positive constants representing the widths of the boundary layers for s_1 and s_2 , respectively. To see the relation of (5) to integral control, observe that inside the boundary layer $\{|s_i| \leq \mu_i\}$, (5) reduces to

$$\begin{aligned} \dot{\sigma}_1 &= e_1 \\ \dot{\sigma}_2 &= k_1^2e_2 + k_2^2\dot{e}_2 + \ddot{e}_2 \end{aligned}$$

which implies that $e_i = 0$ at equilibrium. Thus, (5) represents a ‘conditional integrator’ that provides integral action only inside the boundary layer.

Since

$$\ddot{e}_2 = k_3x_2 - k_4x_3 - d_0 - \phi_d^{(2)}$$

is required to construct s_2 , the parameters k_3, k_4 and d_0 will need to be known. We assume that k_1, k_2 and k_6 are unknown, corresponding to uncertainties in resistance R and inductance L of the phase windings, whereas k_5 , being the number of rotor teeth, is precisely known. Let

$$\theta = [\theta_1, \theta_2, \theta_3]^T = [k_1, k_2, k_6]^T$$

denote the vector of unknown parameters. It can be verified that the expressions for \dot{s}_i take the form

$$\begin{aligned} \dot{s}_1 &= k_0^1(-k_0^1\sigma_1 + \mu_1\text{sat}(s_1/\mu_1)) \\ &\quad + F_1(x, e_1, I_{dd}^{(1)}, \theta) + a_{11}(x, \theta)u_1 \\ \dot{s}_2 &= k_0^2(-k_0^2\sigma_2 + \mu_2\text{sat}(s_2/\mu_2)) \\ &\quad + F_2(x, e_2, \dot{e}_2, \ddot{e}_2, \phi_d^{(3)}, \theta) + a_{22}(x, \theta)u_2 \end{aligned}$$

where

$$\begin{aligned} F_1(\cdot) &= -\theta_1x_1 + k_5x_2x_3 - I_{dd}^{(1)} \\ F_2(\cdot) &= k_1^2\dot{e}_2 + k_2^2\ddot{e}_2 - \phi_d^{(3)} - k_4(k_3x_2 - k_4x_3 - d_0) - k_3\theta_1x_2 \\ &\quad - k_3k_5x_1x_3 - k_3\theta_2x_3 \end{aligned}$$

and $a_{11}(\cdot) = \theta_3, a_{22}(\cdot) = k_3\theta_3$.

The control u is taken as

$$u_i = \frac{-\hat{F}_i(x, e, \varpi) - \beta_i(x, e, \varpi)\text{sat}(s_i/\mu_i)}{\hat{a}_{ii}}, \quad i = 1, 2 \quad (6)$$

where

$$e^T = [e_1, e_2, \dot{e}_2, \ddot{e}_2], \quad \varpi^T = [I_{dd}^{(1)}, \quad \phi_d^{(3)}], \quad \hat{a}_{11}(\cdot) = \hat{\theta}_3,$$

and $\hat{a}_{22}(\cdot) = k_3 \hat{\theta}_3$

$\hat{\theta}_3 > 0$ being a nominal value of θ_3 . To facilitate the discussion, we choose the ‘nominal control component’ $\hat{F}_i(\cdot)$ to cancel all known/nominal terms in $F_i(\cdot)$, that is

$$\begin{aligned} \hat{F}_1(\cdot) &= -\hat{\theta}_1 x_1 + k_5 x_2 x_3 - I_{dd}^{(1)} \\ \hat{F}_2(\cdot) &= k_1^2 \dot{e}_2 + k_2^2 \ddot{e}_2 - \phi_d^{(3)} - k_4(k_3 x_2 - k_4 x_3 - d_0) - k_3 \hat{\theta}_1 x_2 \\ &\quad - k_3 k_5 x_1 x_3 - k_3 \hat{\theta}_2 x_3 \end{aligned}$$

where $\hat{\theta}_1 > 0$ and $\hat{\theta}_2 > 0$ are nominal values of θ_1 and θ_2 , respectively. However, note that other choices of $\hat{F}_i(\cdot)$, including $\hat{F}_i(\cdot) = 0$, are possible.

To make the choice of $\beta_i(\cdot)$ precise, suppose that $\theta_i \in [\theta_i^m, \theta_i^M]$, where $0 < \theta_i^m < \theta_i^M$ and θ_i^m and θ_i^M are known. Let

$$\Delta_i(\cdot) = F_i(\cdot) - (\theta_3/\hat{\theta}_3) \hat{F}_i(\cdot)$$

and $\rho_i(x, e, \varpi)$ be such that

$$\sup \left| \frac{\hat{\theta}_3 \Delta_i(\cdot)}{\theta_3} \right| \leq \rho_i(x, e, \varpi), \quad i = 1, 2$$

where the supremum is taken over all $x, e \in R^4$, $\theta_i \in [\theta_i^m, \theta_i^M]$ and $\varpi \in R^2$. The functions β_i are then chosen as

$$\beta_i(\cdot) = \rho_i(\cdot) + q_i, \quad q_i > 0$$

This choice guarantees that

$$s_i \dot{s}_i < -q_i$$

whenever $|s_i| > \mu_i$, so that the trajectories reach the sets $s_i \leq \mu_i$ in finite time, and stay there thereafter. A standard SMC argument can then be used to prove that the controller (4)–(6) achieves global regulation, provided μ_1 and μ_2 are sufficiently small. In particular, we have the following result. The proof of this theorem for a general MIMO system, stated as [15, Theorem 3.1] and [16, Theorem 2], can be found in either of these two references.

Theorem 1 (Boundedness and error regulation): For any bounded initial state $x(0)$ of the PMSM model (2), the state $x(t)$ of the closed-loop system under the state-feedback control (4)–(6) is bounded for all $t \geq 0$. Moreover, there exists $\mu_i^* > 0$, such that, for $\mu_i \in (0, \mu_i^*]$, $\lim_{t \rightarrow \infty} e(t) = 0$.

A simplification of the design results if we make the choice $\hat{F}_i(\cdot) = 0$, $\beta_i(\cdot) = k_i$, with the constants k_i chosen such that

$$\max \left| \frac{\hat{\theta}_3 F_i(\cdot)}{\theta_3} \right| < k_i, \quad i = 1, 2$$

where the maximisation is taken over all x, e and ϖ in some compact subsets of R^4 and R^2 , respectively, and $\theta_i \in [\theta_i^m, \theta_i^M]$. In this case, the controller is simply

$$u_i = \left(\frac{-k_i}{\hat{a}_{ii}} \right) \text{sat}(s_i/\mu_i) \stackrel{\text{def}}{=} -M_i \text{sat}(s_i/\mu_i), \quad i = 1, 2$$

This design, while having a simple structure, is also natural if the control is required to be bounded, as is the case in real applications, and is a design choice that we will also pursue in the section on output feedback, but for a different reason. For this case, we only have regional results, with the region of attraction determined by constraints on the choice of k_i . If the gains k_i can be chosen sufficiently large, we can achieve semi-global stabilisation. Both these results, along with the global result we mentioned earlier, are covered in [16, Theorem 2].

For the purpose of simulation, we use the following values for the system parameters, obtained from [11]: $R = 19.1388 \Omega$, $L = 40 \text{ mH}$, $K_m = 0.1349 \text{ Nm/A}$, $J = 4.1295 \times 10 \text{ kgm}^2$, $B = 0.0013 \text{ Nm/rad/s}$ and $N_r = 50$. The load torque is assumed to be $\tau_L = 0.2 \text{ kgm}^2/\text{s}^2$. For the purpose of controller design, R and L are assumed to be unknown, with nominal values of $\hat{R} = 20 \Omega$ and $\hat{L} = 35 \text{ mH}$, respectively. Also, $R \in [R^m, R^M]$, with $R^m = 19 \Omega$, and $R^M = 21 \Omega$, and $L \in [L^m, L^M]$, with $L^m = 30 \text{ mH}$, and $L^M = 40 \text{ mH}$. The current reference is taken as $I_{dd}(t) = 0 \text{ A}$ [17]. The values of the controller parameters are taken as $k_0^1 = 20$, $k_0^2 = 100$, $k_1^1 = 7.5 \times 10^4$, $k_2^2 = 550$, $\mu_1 = 0.1$, and $\mu_2 = 50$. Initial values for all the states are taken as zero. The functions $\beta_i(\cdot)$ are taken as

$$\begin{aligned} \beta_1(\cdot) &= [(R^M - \hat{R})|x_1| + (L^M - \hat{L})N_r|x_2x_3| + q_1]/\hat{L}, \\ q_1 &= 2.1 k_0^1 \mu_1 L^M \\ \beta_2(\cdot) &= [(R^M - \hat{R})k_3|x_2| + (L^M - \hat{L})k_1^2 \dot{e}_2 + k_2^2 \ddot{e}_2 \\ &\quad - k_4(k_3 x_2 - k_4 x_3 - d_0) - k_3 k_5 x_1 x_3| + q_2]/\hat{L}, \\ q_2 &= 2.1 k_0^2 \mu_2 L^M \end{aligned}$$

The desired angular position $\phi_d(t) = 0.03142[u(t) + u(t - 0.5)]$, where $u(t)$ is the unit step function. The results of the simulation are shown in Fig. 2. From the figure, it is clear that good tracking performance with very little overshoot is achieved, independent of the magnitude of $\phi_d(t)$.

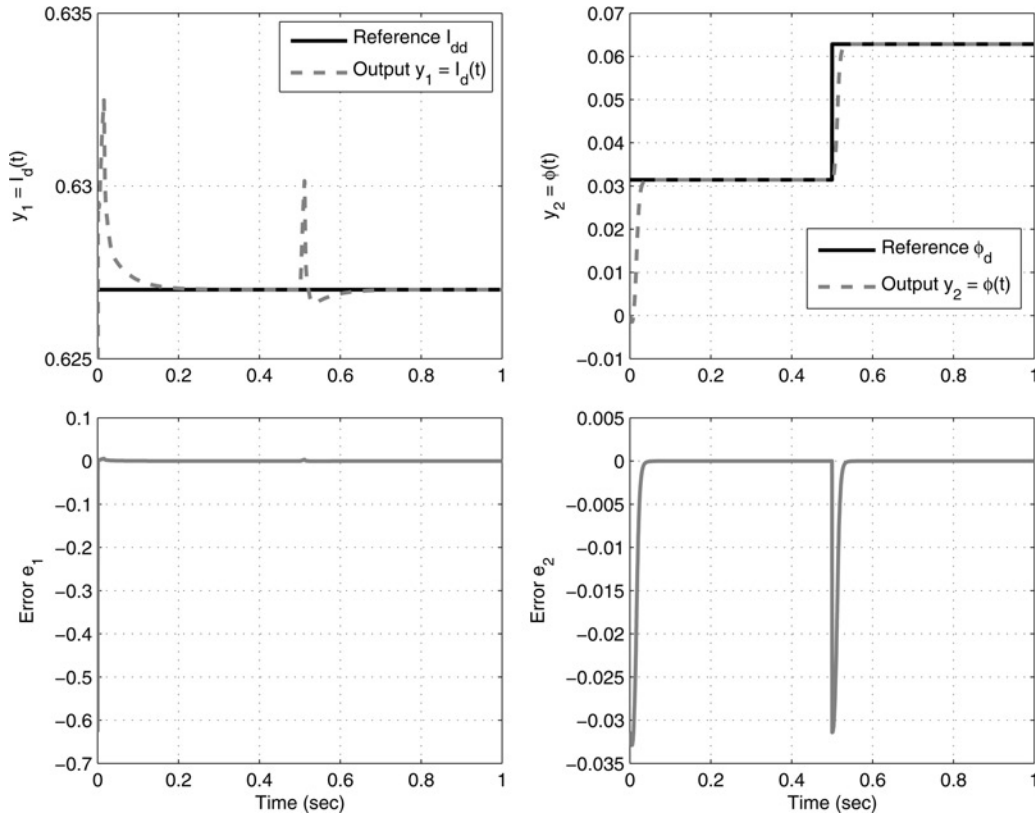


Figure 2 Tracking error performance under state-feedback integral control

In the absence of integral control, it is well known that decreasing the width μ of the boundary layer results in performance that is ‘close’ to that of ideal SMC. The above simulation suggests that this is true with integral control as well, provided the conditional integrator is used. In particular, one can show that the continuous SMC design with conditional integrators ‘recovers the performance’ of the corresponding ideal (discontinuous) SMC without integral control

$$\begin{aligned}
 s_1 &= e_1 \\
 s_2 &= k_1^2 e_2 + k_2^2 \dot{e}_2 + \ddot{e}_2 \\
 u_i &= \frac{-\hat{F}_i(x, e, \varpi) - \beta_i(x, e, \varpi) \operatorname{sgn}(s_i)}{\hat{a}_{ii}}, \quad i = 1, 2 \quad (7)
 \end{aligned}$$

so that we have the following result. As with Theorem 1, this theorem has been stated as [15, Theorem 3.2] and [16, Theorem 3], and the proof of the theorem can be found in either of these references.

Theorem 2 (Performance recovery of ideal SMC): Let $x^*(t)$ be the state of the closed-loop system under the ideal SMC control (7) and $x(t)$ be part of the state of the closed-loop system under the continuous SMC (4)–(6). Then, under the hypotheses of Theorem 1, given any compact subset S of R^4 , with $x^*(0) = x(0) \in S$, there exists

$$\mu_i^* > 0, \text{ such that, } \mu_i \in (0, \mu_i^*] \Rightarrow \|x^*(t) - x(t)\| = O(\|\mu\|) \quad \forall t \geq 0, \text{ where } \mu = [\mu_1, \mu_2]^T.$$

As noted in [12, 15, 16], the state-feedback CSMC with conditional integrators can be thought of as the following two-step modification to ideal SMC:

1. Take $s_i = s_i^* + k_0^i \sigma_i$, where $s_i^* = 0$ is the sliding surface under ideal SMC, and σ_i is the state of the conditional integrator $\dot{\sigma}_i = -k_0^i \sigma_i + \mu_i \operatorname{sat}(s_i/\mu_i)$, $\mu_i, k_0^i > 0$ and μ_i ‘sufficiently small’.
2. Replace $\operatorname{sgn}(s_i^*)$ in ideal SMC with $\operatorname{sat}(s_i/\mu_i)$.

Such a design then recovers the performance of ideal SMC, as stated in Theorem 2. In light of this observation, it becomes imperative to explain the advantage of the proposed technique over ideal SMC. In our design, as a result of inclusion of integral control, we do not require the boundary layer widths μ_1 and μ_2 to be arbitrarily small in order to achieve asymptotic regulation, but only ‘small enough’ to stabilise the equilibrium point (and also small enough for performance recovery of ideal SMC). Consequently, we expect that the method will be less sensitive to the problem of chattering. As a demonstration of this statement, consider a sampled-data implementation of the above controller, that is, we assume that the inputs to the controller are sampled and held signals, with a

zero-order hold, and likewise for the controller outputs. We redo the previous simulation and compare the results against ideal SMC. To simplify the simulation, we exploit the flexibility in the choice of $\hat{F}_i(\cdot)$ and $\beta_i(\cdot)$, and simply design the control as $u_i = -M_i \text{sgn}(s_i)$. For the purposes of simulation, we let $M_1 = 50$, $M_2 = 500$, and the sampling period is assumed to be $T = 0.1$ ms. The results are shown in Fig. 3 (only error e_2 is plotted, since it corresponds to the variable ϕ of physical interest), and we see that asymptotic regulation is lost with the ideal SMC with the sampled-data implementation, and there is considerable chattering in the control v_q . By contrast, asymptotic regulation is retained with the CSMC with conditional integrator, and there is no chattering in the control.

3.2 Output feedback

Suppose that the angular velocity ω of the motor shaft is unavailable for feedback. It is easy to verify that for the system to have a uniform vector relative degree and be transformable to normal form, none of the positive constants k_i and d_0 need to be exactly known. Accordingly, we will assume that in the present case, in addition to the resistance R and inductance L , the parameters K_m , B , J and the load torque τ_L are all unknown, and take the vector θ of unknown parameters as

$$\theta = [k_1, k_2, k_3, k_4, k_6, d_0]^T$$

Since ω is unavailable for feedback, so is $\dot{e}_2 = \omega - \dot{\phi}_d$. Furthermore, even if ω were available for feedback, since $\ddot{e}_2 = k_3 i_q - k_4 \omega - d_0 - \phi_d^2$, and k_3 , k_4 and d_0 are unknown, \ddot{e}_2 would be unavailable for feedback. Therefore, we estimate \dot{e}_2 and \ddot{e}_2 in (4) using the high-gain observer

(HGO) [18]

$$\begin{aligned}\dot{z}_1 &= z_2 + \alpha_1(e_2 - z_1)/\epsilon \\ \dot{z}_2 &= z_3 + \alpha_2(e_2 - z_1)/\epsilon^2 \\ \dot{z}_3 &= \alpha_3(e_2 - z_1)/\epsilon^3\end{aligned}\quad (8)$$

where the positive constants α_1 , α_2 and α_3 are chosen such that the polynomial $\lambda^3 + \alpha_1\lambda^2 + \alpha_2\lambda + \alpha_3$ is Hurwitz. We replace \dot{e}_2 , \ddot{e}_2 and also s_2 in (5) by their estimates z_2 , z_3 , and

$$\hat{s}_2 = k_0^2 \sigma_2 + k_1^2 e_2 + k_2^2 z_2 + z_3 \quad (9)$$

respectively. Finally, motivated in part by the goal of simplifying the design, and in part by the need to work with saturated controls (this is required in order to prevent the peaking phenomenon associated with HGOs [18]), and as mentioned in the previous subsection, we make use of the flexibility in choosing \hat{F}_i , and let $\hat{F}_i = 0$, and simply choose $\beta_i(\cdot)$ as a constant M_i , which is equal to the maximum physically allowable value for the control component $|u_i|$. One can also modify the more general controller (6) for the output-feedback case, without the preceding simplification (10). This essentially requires saturating the control (6) outside a compact set of interest, and the details can be found, for example, in [12, Section 4.2]. With this choice, the final expression for the control then becomes

$$\begin{aligned}u_1 &= -M_1 \text{sat}(s_1/\mu_1) \\ u_2 &= -M_2 \text{sat}(\hat{s}_2/\mu_2)\end{aligned}\quad (10)$$

The results of [12, Theorem 1] show that provided μ_1 , μ_2 and ϵ are 'sufficiently small', and M_1 , M_2 can be chosen 'sufficiently large', the controller (10) can achieve semi-global regulation. Moreover, when M_1 and M_2 are limited

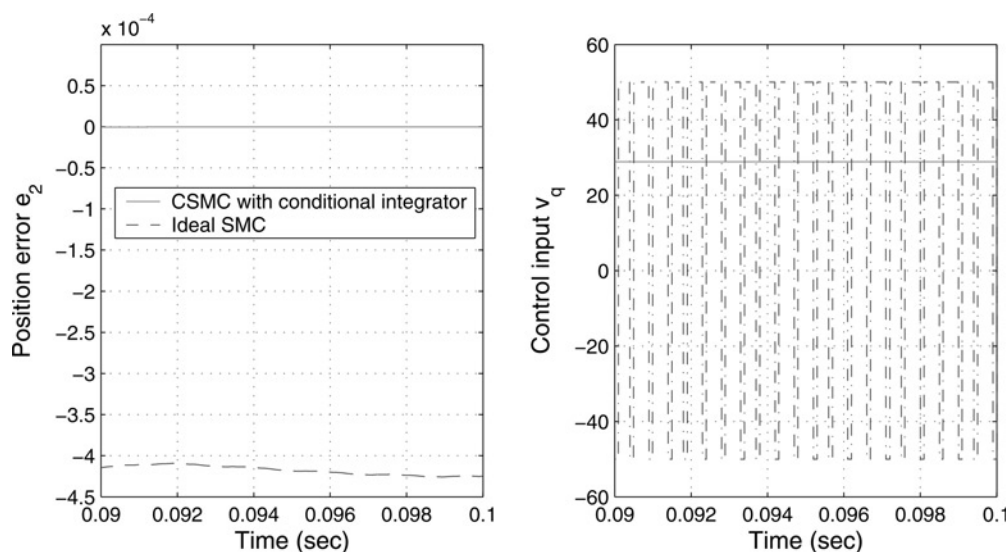


Figure 3 Effect of sampled-time implementation on ideal SMC and CSMC with conditional integrator

in magnitude, there is a trade-off between the control magnitude and the region of attraction. A performance recovery result similar to Theorem 2, which says that the output-feedback CSMC controller with integral action (10) recovers the performance of a corresponding state-feedback ideal SMC, can be found in [12, Theorem 2]. Although a precise statement for the regional case is harder to state without additional terminology (but can be found in [12]), we can state the corresponding results for semi-global regulation and performance recovery, and do so below.

Theorem 3 (Stability and performance): Consider the closed-loop system consisting of the PMSM model (2) and the output-feedback control (4), (5), (8)–(10), and suppose the controller gains M_i can be chosen arbitrarily large. Given compact sets $M \subset R^4$, and $N \subset R^3$ with $e(0) \in M$ and $z(0) \in N$, there exist $\mu_i^* > 0$, such that for each $\mu = [\mu_1, \mu_2]^T$ with $\mu_i \leq \mu_i^*$, there exists $\epsilon^* = \epsilon^*(\mu) > 0$, such that, for $\epsilon \leq \epsilon^*$, all state variables of the closed-loop system are bounded, and $\lim_{t \rightarrow \infty} e(t) = 0$. Furthermore, if $x^*(t)$ be part of the state of the closed-loop system under the ideal state-feedback SMC $u_i = -M_i \text{sgn}(s_i^*)$, and $x(t)$ that with the output-feedback continuous SMC with conditional integrators, with $x(0) = x^*(0)$, then, for every $\tau > 0$, there exists $\mu^* > 0$, and for each μ with $\|\mu\|_\infty \in (0, \mu^*]$, there exists $\epsilon^* = \epsilon^*(\mu) > 0$, such that, for $\mu_i \in (0, \mu_i^*]$ and $\epsilon \in (0, \epsilon^*]$, $\|x(t) - x^*(t)\| \leq \tau \forall t \geq 0$.

For the purpose of simulation, we let $K_m, J, B, N_r, \tau_L, k_0^1, k_0^2, k_1^1, k_1^2, \mu_1, \mu_2$ and I_{dd} retain their values from the previous simulation. Also we take $R = 19.5 \Omega$, $L = 30 \text{ mH}$, and $\phi_d = 0.03142 \text{ rad}$. The HGO gains are taken as $\alpha_1 = 17, \alpha_2 = 80$ and $\alpha_3 = 100$, and the saturation levels for the controls as $M_1 = 50, M_2 = 500$. We compare the performance of the output-feedback controller with the partial state-feedback design

$u_i = -M_i \text{sat}(s_i/\mu_i)$, which makes use of measurements of e_1, e_2, \dot{e}_2 and \ddot{e}_2 . This could, for instance, be the case when the full state x is available for feedback and the parameters k_3, k_4 and d_0 are known. Fig. 4a shows the results of the simulation for $\epsilon = 10^{-4}$, and we see that good tracking performance is achieved by the output-feedback controller, which uses minimal information about the system. Fig. 4b shows the effect of ϵ on the recovery of the state-feedback performance, and it is clear from the figure that the error e_2 under output-feedback approaches the error e_2 under state-feedback as ϵ tends to zero.

4 Conditional servocompensator design

The integral control designs of the previous section was done with the goal of point-to-point motion of the PMSM. In many positioning applications, the desired trajectory for the position is a sinusoid [1]. Specifically, suppose that the desired trajectory asymptotically converges to $\phi_d(t) = r_0 \sin(\omega_0 t)$, which is generated by the neutrally stable exosystem

$$\dot{w} = \begin{bmatrix} 0 & \omega_0 \\ -\omega_0 & 0 \end{bmatrix} w \stackrel{\text{def}}{=} S_0 w, \quad w^T(0) = [0, r_0], \quad r(t) = w_1$$

More general reference trajectories can be considered, as long as they satisfy the conditions of [13, Assumption 3]. We show that the conditional servocompensator design of [13], which is a natural extension of the conditional integrator design of [12], can be applied to this case. Before we proceed further on the control design, we explain the key points briefly. First, by studying the dynamics of the system on the zero-error manifold, a linear internal model is identified, which generates the trajectories of the exosystem, along with a number of higher-order harmonics generated

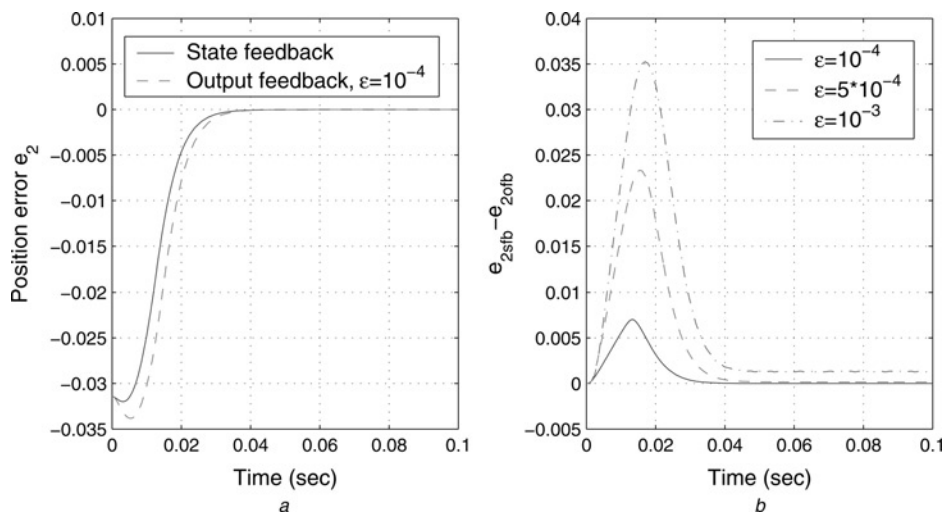


Figure 4 Tracking error performance under the output-feedback integral control
 a State/output feedback integral control
 b Performance recovery of sfb as ϵ tends to zero

by the non-linearities of the system. As before, the idea is to replace ideal discontinuous SMC with a continuous version, but to augment a servocompensator as part of the sliding surface, so as to recover the asymptotic error convergence of ideal SMC. As with the conditional integrator design, the goal is to introduce the servocompensator conditionally, only inside the boundary layer. The reason to do so is as before, namely that a conventional servocompensator design, while guaranteeing steady-state error convergence, does so at the expense of transient performance, while the conditional servocompensator design retains the transient performance of ideal SMC.

To continue with the design, our first goal is to identify a suitable linear internal model that generates the steady-state values of the control inputs v_d and v_q . As before, the desired reference for the current i_d is a constant I_{dd} . It can be verified that with steady-state values $x_{1ss}(t) = I_{dd}$ and $x_{4ss}(t) = r_0 \sin(\omega_0 t)$, respectively, for x_1 and x_4 , the steady-state values of x_2 and x_3 are given by

$$x_{2ss} = [d_0 + k_4 r_0 \omega_0 \cos(\omega_0 t) - r_0 \omega_0^2 \sin(\omega_0 t)]/k_3$$

$$\text{and } x_{3ss} = r_0 \omega_0 \cos(\omega_0 t)$$

respectively, and the steady-state values of the control inputs v_d and v_q are given by

$$u_{1ss} = \gamma_1 + \gamma_2 \cos(\omega_0 t) + \gamma_3 \sin(2\omega_0 t) + \gamma_4 \cos(2\omega_0 t)$$

$$u_{2ss} = \gamma_5 + \gamma_6 \sin(\omega_0 t) + \gamma_7 \cos(\omega_0 t)$$

for some constants γ_1 to γ_7 . The steady-state values of the control u_{iss} satisfy identities of the form

$$L_s^q \chi = c_0 \chi + c_1 L_s \chi + \dots + c_{q-1} L_s^{q-1} \chi \quad (11)$$

where $L_s \chi = (\partial \chi / \partial w) S_0 w$, and the (characteristic) polynomial

$$\lambda^q - c_{q-1} \lambda^{q-1} - \dots - c_0$$

has distinct roots on the imaginary axis. In particular, u_{1ss} does so with $q = 5$, $c_0 = 0$, $c_1 = -4\omega_0^4$, $c_2 = 0$, $c_3 = -5\omega_0^2$ and $c_4 = 0$, whereas u_{2ss} does so with $q = 3$, $c_0 = 0$, $c_1 = -\omega_0^2$ and $c_2 = 0$. An explanation of the identity (11) can be found in the paragraph following [13, Assumption 5]. Roughly speaking, it guarantees the existence of a linear internal model that generates the trajectories of the exosystem, along with a number of higher-order deformations that result from the plant non-linearities. Let

$$S_1 = \begin{bmatrix} 0 & 1 & 0 & 0 & 0 \\ 0 & 0 & 1 & 0 & 0 \\ 0 & 0 & 0 & 1 & 0 \\ 0 & 0 & 0 & 0 & 1 \\ 0 & -4\omega_0^4 & 0 & -5\omega_0^2 & 0 \end{bmatrix}, \quad S_2 = \begin{bmatrix} 0 & 1 & 0 \\ 0 & 0 & 1 \\ 0 & -\omega_0^2 & 0 \end{bmatrix}$$

be the internal model matrices corresponding to u_{1ss} and u_{2ss} , and

$$J_1 = [0 \ 0 \ 0 \ 0 \ 1]^T, \quad J_2 = [0 \ 0 \ 1]^T$$

It can be verified that the steady-state control inputs $u_{iss} = \chi_i$ are generated by the internal models $(\partial \tau_i / \partial w) S_0 w = S_i \tau_i$, $x_i = \Gamma_i \tau_i$, where $\tau = [\chi_i L_s \chi_i \dots L_s^{q-2} \chi_i L_s^{q-1} \chi_i]^T$, and $\Gamma_i = [10 \dots 0]_{1 \times q}$. We take σ_1 and σ_2 as outputs of the conditional servocompensators

$$\dot{\sigma}_i = (S_i - J_i K_0^i) \sigma_i + \mu_i J_i \text{sat}(\hat{s}_i / \mu_i) \quad (12)$$

where

$$s_1 = K_0^1 \sigma_1 + e_1$$

$$s_2 = K_0^2 \sigma_2 + k_1^2 e_2 + k_2^2 \dot{e}_2 + \ddot{e}_2 \quad (13)$$

The matrices K_0^i are chosen such that $S_i - J_i K_0^i$ are Hurwitz (which is always possible since the pair (S_i, J_i) is controllable), the scalars k_1^2 and k_2^2 are chosen such that the polynomial $x^2 + k_2^2 x + k_1^2$ is Hurwitz, $\hat{s}_1 = s_1$, $\hat{s}_2 = K_0^2 \sigma_2 + k_1^2 e_2 + k_2^2 \dot{e}_2 + \ddot{e}_2$, where z_2 and z_3 are estimates of \dot{e}_2 and \ddot{e}_2 , respectively, provided by the high-gain observer (8).

As with the conditional integrator design, (12) represents a perturbation of the exponentially stable system $\dot{\sigma} = (S - JK_0)\sigma$, with the norm of the perturbation bounded by the small parameter μ , and therefore $\|\sigma_i\| = O(\mu_i)$, provided $\sigma_i(0) = O(\mu_i)$. With state feedback, (i.e. when $\hat{s} = s$) inside the boundary layer $|s| \leq \mu$, (12) reduces to $\dot{\sigma} = S\sigma + J e_a$, where the 'augmented error' e_a is a linear combination of the tracking error and its derivatives, and it is clear that it generates the steady-state trajectories when $e_a = 0$, that is, provides servo-action inside the boundary layer.

To continue with the design, the control then is taken as in (10), that is

$$u_i = -M_i \text{sat}(\hat{s}_i / \mu_i) \quad (14)$$

As before, we can choose the nominal component of the control to be non-zero, and possibly error dependent, and also choose the 'switching' component as state/error dependent. We do not pursue that design here for the sake of simplicity. This completes the design of the controller. Analytical results for stability and performance of the controller (12)–(14), similar to the ones in the previous section, can be found in [13, Theorems 1 and 2], and are stated in Theorem 3 below for the special semi-global regulation case.

Theorem 4 (Stability and performance): Consider the closed-loop system consisting of the PMSM model (2) and the output-feedback control (12)–(14), and suppose the controller gains M_i can be chosen arbitrarily large. Given compact sets $M \subset R^4$, and $N \subset R^3$ with $e(0) \in M$ and $z(0) \in N$, there exist $\mu_i^* > 0$, such that for each $\mu = [\mu_1, \mu_2]^T$ with $\mu_i \leq \mu_i^*$, there exists $\epsilon^* = \epsilon^*(\mu) > 0$, such that, for $\epsilon \leq \epsilon^*$, all state variables of the closed-loop system are bounded, and $\lim_{t \rightarrow \infty} e(t) = 0$. Furthermore, if $x^*(t)$ be part of the state of the closed-loop system under the ideal state-feedback SMC $u_i = -M_i \text{sgn}(s_i^*)$, and $x(t)$ that with the output-feedback continuous SMC with conditional servocompensators (12), with $x(0) = x^*(0)$, and $\sigma_i(0) = 0$. Then, for every $\tau > 0$, there exists $\mu^* > 0$, and for each μ with $\|\mu\|_\infty \in (0, \mu^*]$, there exists $\epsilon^* = \epsilon^*(\mu) > 0$, such that, for $\mu_i \in (0, \mu^*]$ and $\epsilon \in (0, \epsilon^*]$, $\|x(t) - x^*(t)\| \leq \tau \forall t \geq 0$.

In order to demonstrate the efficacy of the design by simulation, we repeat the simulation in Section 3.2, with all the numerical values retained, except for the reference $\phi_d(t)$, which is now chosen as $\phi_d(t) = r_0 \cos(\omega_0 t)$. This is a sinusoidal signal that is simply phase-shifted from $\phi_d(t) = r_0 \sin(\omega_0 t)$ by $\pi/2$, and chosen this way to have a non-zero initial error $e_2(0)$. Two sets of values of (r_0, ω_0) are used in the simulation, $(r_0, \omega_0) = (\pi/2, 2)$ and $(r_0, \omega_0) = (\pi/10, 5)$. The matrices K_0^i in the conditional servocompensator (12) are chosen to place the eigenvalues of $S_1 - J_1 K_0^1$ and $S_2 - J_2 K_0^2$ at $\{-1, -2 \pm j, -3 \pm j\}$ and $\{-1, -2 \pm j\}$, respectively. We compare the performance against a continuous SMC design that does not include a servocompensator, that is, $\hat{s}_1 = e_1$, $\hat{s}_2 = k_1^2 e_2 + k_2^2 z_2 + z_3$, where z_2 and z_3 are as defined above, and $u_i = -M_i \text{sat}(\hat{s}_i / \mu_i)$. The results of the simulation are shown in Fig. 5, and we see that good tracking performance is achieved by the output-feedback servocompensator design, which uses minimal information about the system. As expected, the transient performance of the continuous SMC without servocompensator is close to the one with a servocompensator (indistinguishable in the figure), but the steady-state error is non-zero without servocompensation, whereas it tends to zero with the conditional servocompensator.

In our simulations so far, we have assumed that the load torque τ_L is constant. This assumption can be relaxed: (i) for the constant exogenous signals case, since we only require that τ_L be asymptotically constant, and $\phi(t)$ and $\omega(t)$ approach a constant and zero, respectively, we can allow $\tau_L = f_\tau(\phi(t), \omega(t))$, where $f_\tau(\cdot)$ is a sufficiently smooth function of its arguments, and (ii) for the sinusoidal exogenous signals case, on account of the need for the identity of the form (11) that the steady-state control must satisfy, it can be verified that $f_\tau(\cdot)$ will have to be a polynomial function of its inputs, and that its form must be known, that is

$$f_\tau(\phi, \omega) = \sum_{i \in I, j \in J} \alpha_{ij} \phi^i \omega^j$$

where $I, J \subset Z_{\geq 0}$ known, and α_{ij} possibly unknown.

4.1 Internal model perturbations

In the sinusoidal exogenous signals case, when the polynomial condition is violated, for example, when the load torque is of the form $\tau_L = N \sin(\phi)$ say, then, as shown in [13, Section 5], polynomial approximations may be used to achieve practical regulation of the error. Successively higher-order approximations will lead to better approximations that make the steady-state error smaller (see [13, Theorem 3] for a precise statement about the effect of ‘size’ of internal model perturbations on the steady-state error), but will require successively higher-order servocompensator designs. Ideal SMC does not require such approximations, but suffers from chattering. Replacing the discontinuous control with a continuous approximation that does not include a servocompensator will result in steady-state errors that are $O(\mu)$, so that we need to make μ smaller in order to decrease the steady-state error, but a too small μ will lead to chattering again. The error can be made smaller by incorporating a servocompensator that is based on polynomial approximations. However, when a conventional servocompensator driven by the tracking error of the form

$$\dot{\sigma}_i = S_i \sigma_i + J_i e_i$$

is used, then, as previously mentioned, although successively higher-order approximations will result in smaller steady-state errors, this will be at the expense of degraded transient performance, which becomes progressively worse as the order of the approximation increases. The transient response of the conditional servocompensator design, on the other hand, is practically independent of the servocompensator order, and, as shown by Theorem 4, is simply close to an ideal SMC design that does not include a servocompensator.

In order to illustrate the above observations, we repeat the previous simulation, but with the following changes: we assume that the load torque is $\tau_L = N \sin(\phi)$, where (as in [8]) $N = 1.7201 \text{ kg m}^2/\text{s}^2$, and the desired reference trajectory is, as before, $\phi_d(t) = r_0 \cos(\omega_0 t)$ with $r_0 = 1$, $\omega_0 = 2$. It is easy to verify that the steady-state values of the control inputs v_d and v_q are given by

$$\begin{aligned} u_{1ss} &= \gamma_8 + \gamma_9 \sin(2\omega_0 t) + \gamma_{10} \cos(2\omega_0 t) + \gamma_{11} \cos(\omega_0 t) \\ &\quad \times \sin(\sin(\omega_0 t)) \\ u_{2ss} &= \gamma_{12} \sin(\omega_0 t) + \gamma_{13} \cos(\omega_0 t) + \gamma_{14} \sin(\sin(\omega_0 t)) \\ &\quad + \gamma_{15} \cos(\omega_0 t) \cos(\sin(\omega_0 t)) \end{aligned}$$

for some constants γ_8 to γ_{15} , and it can be verified that these do not satisfy identities of the form (11). Consequently, we replace $\sin(\sin(\omega_0 t))$ and $\cos(\sin(\omega_0 t))$ (that appear in the terms with constant coefficients γ_{11} , γ_{14} and γ_{15}) with polynomial approximations. In particular, viewing $\sin(\omega_0 t)$

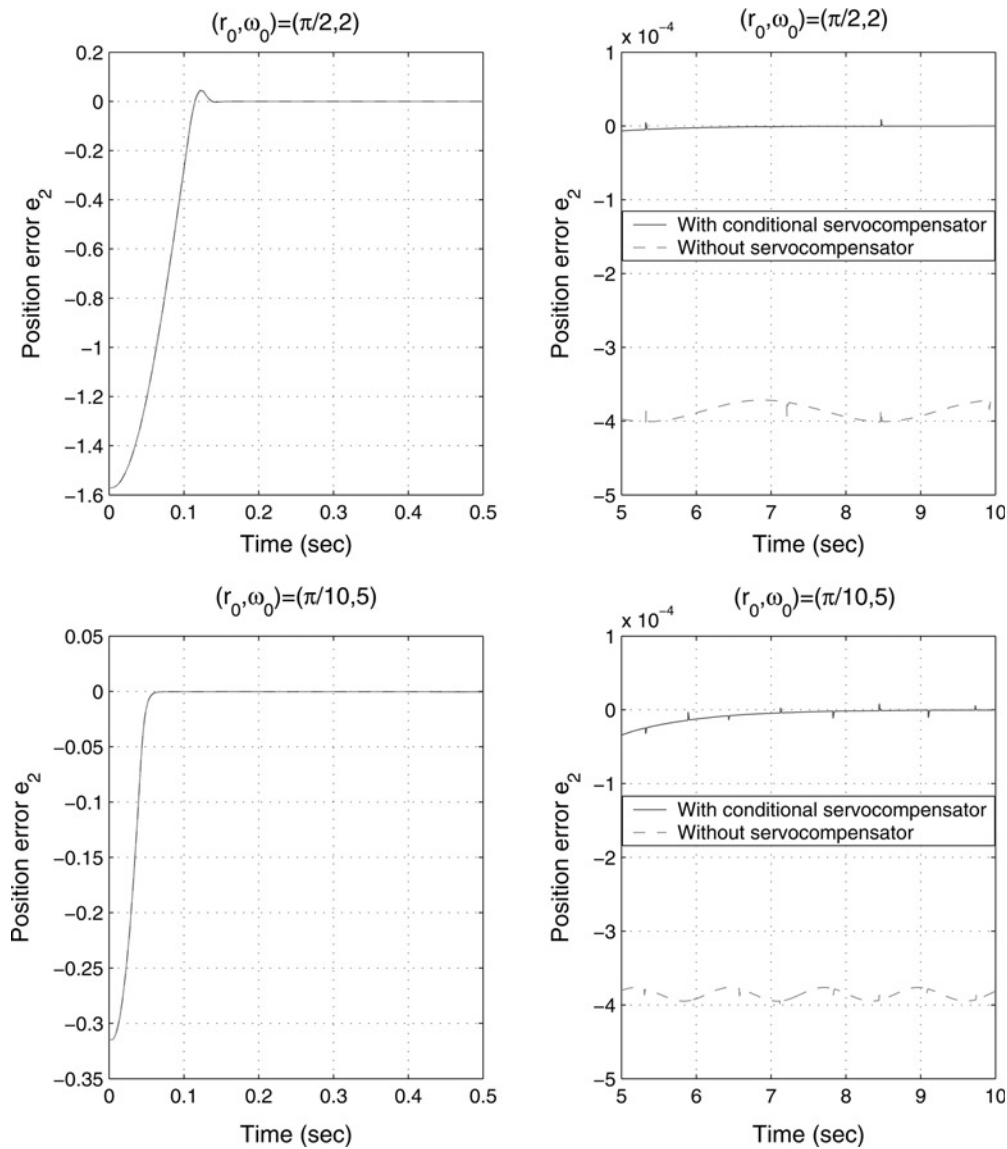


Figure 5 Sinusoidal reference tracking using output-feedback servocompensators

as the argument ϑ of $\sin(\vartheta)$ and $\cos(\vartheta)$, we employ the following two approximations:

1. *Approximation 1:* $\sin(\vartheta) \simeq \vartheta, \quad \cos(\vartheta) \simeq 1$
2. *Approximation 2:* $\sin(\vartheta) \simeq \vartheta - \vartheta^3/3, \quad \cos(\vartheta) \simeq 1 - \vartheta^2/2$

It is then straightforward to verify that that the internal model matrices S_i corresponding to these two approximations then are:

Approximation 1

$$S_1 = \begin{bmatrix} 0 & 1 & 0 \\ 0 & 0 & 1 \\ 0 & -4\omega_0^2 & 0 \end{bmatrix}, \quad S_2 = \begin{bmatrix} 0 & 1 \\ -\omega_0^2 & 0 \end{bmatrix}$$

Approximation 2

$$S_1 = \begin{bmatrix} 0 & 1 & 0 & 0 & 0 \\ 0 & 0 & 1 & 0 & 0 \\ 0 & 0 & 0 & 1 & 0 \\ 0 & 0 & 0 & 0 & 1 \\ 0 & -64\omega_0^4 & 0 & -20\omega_0^2 & 0 \end{bmatrix},$$

$$S_2 = \begin{bmatrix} 0 & 1 & 0 & 0 \\ 0 & 0 & 1 & 0 \\ 0 & 0 & 0 & 1 \\ -9\omega_0^4 & 0 & -10\omega_0^2 & 0 \end{bmatrix}$$

For the first (lower-order) approximation, the matrices K_0^i in the conditional servocompensator design are chosen to place

the eigenvalues of $S_1 - J_1 K_0^1$ and $S_2 - J_2 K_0^2$ at $\{-1, -2 \pm j\}$ and $\{-1, -2\}$, respectively. For the second (higher-order) approximation, these are chosen to place the eigenvalues of $S_1 - J_1 K_0^1$ and $S_2 - J_2 K_0^2$ at $\{-1, -2 \pm j, -5 \pm j\}$ and $\{-2 \pm j, -5 \pm j\}$, respectively. The conventional servocompensator design requires a complete redesign of the sliding surface parameters (the details of which can be found in [19]), and we only mention that in order to make a meaningful comparison, the controller parameters in the simulation results that we present were chosen so that the eigenvalues from the conditional design are retained.

The results of the simulation are shown in Fig. 6, with variables q_1 and q_2 indicated being the orders of matrices S_1 and S_2 , respectively. The set $q_1 = 3, q_2 = 2$ corresponds to the lower-order polynomial approximation, whereas $q_1 = 5, q_2 = 4$ to the higher-order one. Several inferences can be made from the figure. The subplots in the first row show that the steady-state errors decrease as the polynomial approximation order increases (i.e. the approximation

becomes better), both for the conditional and for the conventional servocompensator design. Furthermore, the steady-state errors for the same approximation order are comparable in both these designs. From the subplots on the second row, we see, as expected, that the transient performance of the conditional servocompensator designs is close to that of the continuous SMC without servocompensator (indistinguishable in the figure) and hence to that of an ideal SMC, regardless of the order of the servocompensator (which are shown with $q_2 = 2$ and $q_2 = 4$). In other words, increase in servocompensator order does not degrade the transient performance of the design. The steady-state error is non-zero without servocompensation, whereas it decreases (significantly) with the servocompensator (shown for $q_2 = 2$). The subplot on the last row clearly demonstrates the advantage of the conditional design over a conventional one. In particular, while the steady-state performance of the two designs are comparable (as seen from the subplots in the first row), increasing the order of the servocompensator in order to decrease the steady-state error has the drawback of

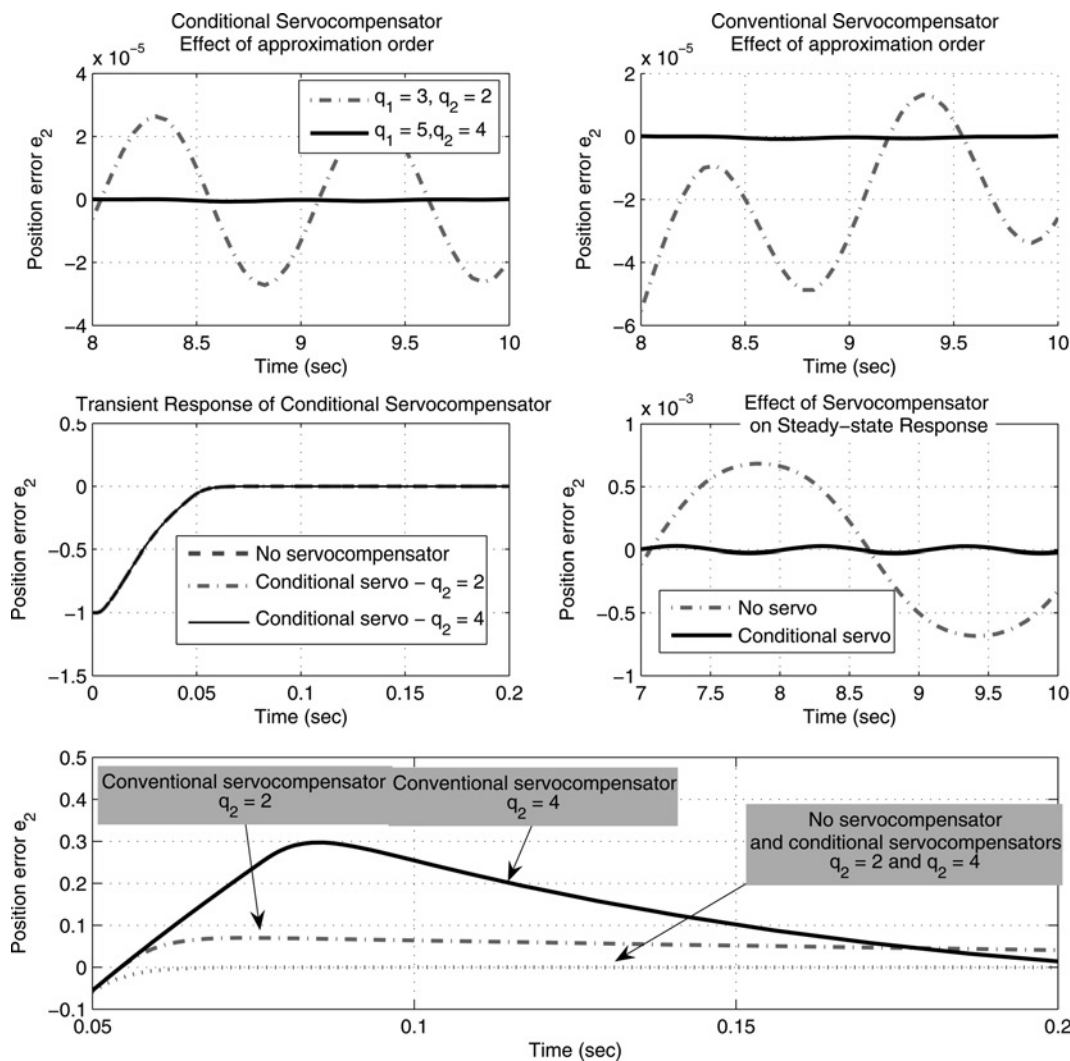


Figure 6 Effect of increasing approximation orders on transient and steady-state performance

degrading the transient response in the conventional design, which clearly gets progressively worse as the servocompensator order increases. The conditional servocompensator design's transient performance though, as we have just observed, is practically independent of the servocompensator order.

5 Conclusions

In this paper, we presented a new approach for position control of a permanent magnet stepper motor. Our problem formulation allows for the system to contain constant unknown parameters θ , and time-varying matched disturbances $\delta(t)$ that could also possibly depend on θ and the state x . In the case of constant exogenous signals, we looked at both a state-feedback design for global regulation, and an output-feedback design for regional/semi-global regulation, based on conditional integrators and sliding mode control. An extension of the design to the case of sinusoidal references using conditional servocompensators was provided, with both state- and output-feedback designs being possible. Analytical results for stability and performance of the proposed method were provided, with the performance of ideal SMC as the benchmark. Simulation results show that good tracking performance is achieved in all cases, in spite of partial knowledge of the machine parameters. Advantages of the design over ideal SMC as regards the issue of chattering and over conventional servocompensator design as regards transient performance were also demonstrated by simulation. Lastly, although we specifically considered PMSMs in this paper, our results can be extended to other types of motors, such as permanent magnet synchronous and DC motors.

6 Acknowledgments

The author would like to thank Prof. H. K. Khalil for his valuable guidance and his contributions to a preliminary version of this manuscript. This work was supported in part by a grant from the San Diego State University Foundation. A preliminary version of this paper was presented at the 2005 American Control Conference [14].

7 References

- [1] DAWSON D.M., HU J., BURG T.C.: 'Nonlinear control of electric machinery', Control Engineering Series (Marcel Dekker, Inc., New York, 1998)
- [2] ZRIBI M., CHIASSON J.N.: 'Position control of a PM stepper motor by exact linearization', *IEEE Trans. Autom. Control*, 1991, **36**, pp. 620–625
- [3] BODSON M., CHIASSON J.N., NOVOTNAK R.T., REKOWSKI R.B.: 'High performance nonlinear feedback control of a permanent

magnet stepper motor', *IEEE Trans. Control Syst. Technol.*, 1993, **1**, (1), pp. 5–14

- [4] CHIASSON J.N., NOVOTNAK R.T.: 'Nonlinear speed observer for the PM stepper motor', *IEEE Trans. Autom. Control*, 1993, **38**, pp. 1584–1588
- [5] BURG T.C., HU J., DAWSON D.M., VEDAGARBHA P.: 'A global exponential position tracking controller for a permanent magnet stepper motor via output feedback'. Proc. third IEEE Conf. Control Applications, 1994, pp. 213–218
- [6] KHORRAMI F., KRISHNAMURTHY P., MELKOTE H.: 'Modeling and adaptive nonlinear control of electric motors' (Springer, New York, 2003)
- [7] KRISHNAMURTHY P., KHORRAMI F.: 'Permanent magnet stepper motor control via position-only feedback', *IEE Proc. Control Theory Appl.*, 2004, **151**, (4), pp. 499–510
- [8] KRISHNAMURTHY P., KHORRAMI F.: 'Robust adaptive voltage-fed permanent magnet stepper motor control without current measurements', *IEEE Trans. Control Syst. Technol.*, 2003, **11**, pp. 415–425
- [9] MELKOTE H., KHORRAMI F.: 'Nonlinear output feedback control for stepper motors: a robust adaptive approach'. Proc. IEEE Conf. Control Applications, 1999, pp. 755–760
- [10] MARINO R., PERESADA S., TOMEI P.: 'Nonlinear adaptive control of permanent magnet stepper motors', *Automatica*, 1995, **31**, (11), pp. 1595–1604
- [11] ZRIBI M., SIRA-RAMIREZ H., NGAI A.: 'Static and dynamic sliding mode control schemes for a PMSM', *Int. J. Control*, 2001, **74**, (2), pp. 103–117
- [12] SESHAGIRI S., KHALIL H.K.: 'Robust output feedback regulation of minimum-phase nonlinear systems using conditional integrators', *Automatica*, 2005, **41**, (1), pp. 43–54
- [13] SESHAGIRI S., KHALIL H.K.: 'Robust output feedback regulation of minimum-phase nonlinear systems using conditional servocompensators', *Int. J. Robust Nonlinear Control*, 2005, **15**, (2), pp. 83–102
- [14] SESHAGIRI S., KHALIL H.K.: 'Position control of a PMSM using conditional integrators'. 2005 American Control Conf., Portland, OR, USA, June 2005
- [15] SESHAGIRI S.: 'Robust output regulation of minimum phase nonlinear systems using conditional servocompensators'. PhD thesis, Michigan State University E.Lansing, USA, 2003

[16] SESHAGIRI S., KHALIL H.K.: 'On introducing integral action in sliding mode control'. Proc. IEEE Conf. Decision and Control, 2002

[17] LAGHROUCHE S., PLESTAN F., GLUMINEAU A., BOISLIVEAU R.: 'Robust second order sliding mode control for a permanent magnet synchronous motor'. Proc. American Control Conf., 2003, pp. 4071–4076

[18] ESFANDIARI F., KHALIL H.K.: 'Output feedback stabilization of fully linearizable systems', *Int. J. Control*, 1992, **56**, pp. 1007–1037

[19] KHALIL H.K.: 'On the design of robust servomechanisms for minimum phase nonlinear systems', *Int. J. Robust Nonlinear Control*, 2000, **10**, pp. 339–361